**International Journal of Research in Science & Engineering**
**ISSN: 2394-8299**
Vol: 01, No. 02, Oct-Nov 2021
http://journal.hmjournals.com/index.php/IJRISE
**DOI:** https://doi.org/10.55529/ijrise.12.1.24

# Analysis of Microbial Growth Models for Microorganisms in Chicken Manure Digester

**Abdulhalim Musa Abubakar[1,*], Zahra Soltanifar[2], Yusufu Luka[3], Eme William Udoh[4], Mamoudou Hamadou[5]**

*[1*,3]Department of Chemical Engineering, Faculty of Engineering, Modibbo Adama University (MAU), PMB 2076, Yola, Adamawa State, Nigeria*
*[2]Department of Fisheries, College of Agriculture and Natural Resources, University of Tehran, Karaj, Iran*
*[4]Science Laboratory Technology (SLT), Microbiology, Akwa Ibom State Polytechnic, Ikot Osurua, Nigeria*
*[5]Department of Biological Sciences, Faculty of Science, University of Maroua, Cameroon*

*Corresponding Email: [1*]abdulhalim@mau.edu.ng*

**Received:** 03 August 2021 **Accepted:** 20 October 2021 **Published:** 19 November 2021

***Abstract:*** ***Several microorganisms are there in chicken manure (CM) but Salmonella, Cryptosporidium and Escheridia coli are the most identified. Objective of this research includes, carrying out microbial count in the CM substrate for 40 days retention time in a digester, uterlizing kinetic expressions satisfying the process and fitting results obtained with 26 existing microbial growth kinetic models. Results shows that microbes inside the CM slurry, survived for a full period of 37 days divided into 7 days of acclimatization, 23 days of growth and another 7 days of equal rate of death and multiplication. Findings shows that the maximum specific growth rate, $\mu_{max}$, estimated from the basic Monod equation, of the organisms is 0.0076hr$^{-1}$ and the half-saturation constant, $K_s$, is 3.838× 〖10〗 ^8 mg/l which indicates how sufficient the substrate concentration is for the bacteria to feed on. Not all 26 growth kinetic models found in the literature fit the measured experimental data. However, Monod with decay rate, Wayman and Tseng, Han and Levenspiel, Luong and Moser models fit the Monod values after regressing with POLYMATH 6.10 Educational Release.***

***Keywords:*** ***Chicken Manure, Microbial Growth Models, Monod, Kinetic Study, Serial Dilution, Kinetic Parameter, Anaerobic Digestion, Biogas.***

## 1. INTRODUCTION

Presently, there are three models that have been used consistently to describe the kinetics of the anaerobic decomposition of substrate including CM. They are growth kinetics, kinetics of

**International Journal of Research in Science & Engineering**
**ISSN: 2394-8299**
Vol: 01, No. 02, Oct-Nov 2021
http://journal.hmjournals.com/index.php/IJRISE
**DOI:** https://doi.org/10.55529/ijrise.12.1.24

biogas production, and kinetics of substrate degradation models, among which kinetics of biogas production is the most important (Van et al., 2018). In CM, there are mostly three types of micro-organisms, namely, Salmonella spp., Escherichia coli (E. coli), and Cryptosporidium. Salmonella is a non-spore forming, gram-negative, and rod-shaped bacterium (Hawkins et al., 2019). It is the most common foodborne diseases (Hawkins et al., 2019; Veys et al., 2016) with eggs being the main sources of Salmonella enteritidis infections in humans. They survive and grow in low-moisture foods (e.g. egg whites), under a favourable temperature range and is often difficult to control (Kang et al., 2021). Colonies of Salmonella cells are often identified as having a dark centre and clear circles (Xu et al., 2018) and size ranges from 1.7-6.16$\log_{10}$ CFU/g in chicken litter of 3.5kg according to research carried out by Pal et al. (2014). E. coli is a rod-shaped, gram negative, motile and facultative bacterium, resident in colons or intestinal flora of mammalian or warm-blooded animals (Cho et al., 2018; Elbing & Brent, 2020; Li et al., 2021). Though, most strains are harmless, some strains are reliable indicators of faecal pollution, urinary tract infections, severe food-borne disease, bloodstream infection (BSI), watery diarrhoea, meningitis, sepsis and, abdominal infections (Cho et al., 2018; Hossain et al., 2017; Li et al., 2021). E. coli grow on mediums supplying the cells with vitamins, glucose, salts, trace metals, amino acids, carbon, nitrogen, phosphorus, nucleotide precursors and, other metabolites (Elbing & Brent, 2020). It is the most common hospital-acquired pathogen growing on eosin methylene blue (EMB) agar (Chen & Jiang, 2014; Hossain et al., 2017; Li et al., 2021). Thomas et al. (2019) in their work counted 7$\log_{10}$ CFU/ml of E. coli in CM, though $10^5$-$10^{10}$CFU$g^{-1}$ of E. coli in pathogenic straws had been reported by Kyakuwaire et al. (2019) in their work. Cryptosporidium spp., where 31 species and > 40 genotypes are available, are common causes of food- and water-borne diarrheal illnesses such as gastrointestinal disease, found mainly in human and animal faeces including poultry birds (Kyakuwaire et al., 2019; Li et al., 2021; Widmer et al., 2020). The totality or types of microorganisms that could be present in CM are bacteria (e.g. Campylobacter, E. coli, Mycobacterium, Listeria, Staphylococcus, Salmonella, Clostridium, Streptococcus, Actinobacillus, Globicatella, Bordetalla, lactic acid bacteria and coliform bacteria of weight ranging from $10^6$-$10^8$CFU$g^{-1}$), protozoa such as Giardia spp. and Cryptosporidium, fungi, helminthes and viruses (Huang et al., 2020; Thomas et al., 2019; Tuyarum et al., 2019). In general, microbial concentration in chicken litter is capable of reaching up to $10^{10}$CFU/g (Chen & Jiang, 2014).

During anaerobic batch fermentation of CM, these microorganisms grow under a variety of physical, chemical, and nutritional conditions. They do this, by extracting nutrients from the medium (CM slurry) and converting them into biological compounds. This changes is accomplished through a cell's use of a number of dissimilar enzymes in a strings of reactions to produce metabolic products, which either remain in the cell (intracellular), providing the cell with energy or be secreted from the cells (extracellular) as bioproducts (Liu, 2017). Growth therefore, is believed to mean, both replication of cells and change in cell size. The growth and multiplication of bacteria in controlled environments, thus arouse the interest of microbiologists, biochemical engineers and, cell-growth experts, as they instigate bioprocess simulation and control scheme design (González-figueredo et al., 2018). Objective of this research is to carry out live cell count in the CM substrate for 40 days retention period in a

**International Journal of Research in Science & Engineering**
**ISSN: 2394-8299**
Vol: 01, No. 02, Oct-Nov 2021
http://journal.hmjournals.com/index.php/IJRISE
**DOI:** https://doi.org/10.55529/ijrise.12.1.24

bench-scale digester, identify kinetic equations governing the process and fit results obtained with existing microbial growth kinetic models.

## 2. MODEL DESCRIPTION

### 2.1. Existing Growth Kinetics

Over the years, several microbial growth kinetic models had been proposed. Table 1 depicts 26 models developed to analyse growth characteristics in batch bioreactors.

Table 1. Specific Growth Rate Models

| S/No. | Model Name | Expression | Reference |
|---|---|---|---|
| 1. | Monod | $\mu = \frac{\mu_{max} S}{K_s + S}$ | (Abubakar et al., 2017; Dlangamandla et al., 2019; Shariful Islam et al., 2021) |
| 2. | Monod with Decay rate | $\mu = \frac{\mu_{max} S}{K_s + S} - b$ | (Abubakar et al., 2017) |
| 3. | Contois | $\mu = \frac{\mu_{max} S}{K_s X + S}$ | (Annuar et al., 2008) |
| 4. | Contois with Decay rate | $\mu = \frac{\mu_{max} S}{K_s X + S} - b$ | (Abubakar et al., 2017) |
| 5. | Andrew | $\mu = \frac{\mu_{max}}{1 + \frac{K_s}{S} + \frac{S}{K_i}}$ | (González-figueredo et al., 2018; Xu et al., 2018) |
| 6. | Andrew with Decay rate | $\mu = \frac{\mu_{max}}{1 + \frac{K_s}{S} + \frac{S}{K_i}} - b$ | (Abubakar et al., 2017) |
| 7. | Moser Model | $\mu = \frac{\mu_{max} S^n}{K_s + S^n}$ | (Muloiwa et al., 2020) |
| 8. | Teissier | $\mu = \mu_{max}\left(1 - e^{-S/K_s}\right)$ | (Halmi et al., 2014) |
| 9. | Halden | $\mu = \frac{\mu_{max} S}{K_s + S + \frac{S^2}{K_i}}$ | (Bayen et al., 2018) |
| 10. | Haldane | $\mu = \frac{\mu_{max} S}{(K_s + S)\left(1 + \frac{S}{K_i}\right)}$ | (Bayen et al., 2018; Muloiwa et al., 2020; Xu et al., 2018) |
| 11. | Verhulst | $\mu = \mu_{max}\left(1 - \frac{X}{X_m}\right)$ | (Shariful Islam et al., 2021; |

**International Journal of Research in Science & Engineering**
**ISSN: 2394-8299**
Vol: 01, No. 02, Oct-Nov 2021
http://journal.hmjournals.com/index.php/IJRISE
**DOI:** https://doi.org/10.55529/ijrise.12.1.24

| | | | |
|---|---|---|---|
| | | | UlukardeŞler & Atalay, 2018) |
| 12. | Powell | $\mu = \mu_{max} \frac{1 + \frac{S}{K_s} + \propto}{2 \propto} \left[ 1 - \left\{ 1 - \frac{4 \propto \frac{S}{K_s}}{\left(1 + \frac{S}{K_s} + \propto\right)^2} \right\}^{1/2} \right]$ | (Shariful Islam et al., 2021; UlukardeŞler & Atalay, 2018) |
| 13. | Dabes | $\mu = \mu_{max} \frac{1 + \frac{S}{K_s} + \propto}{4 \propto} \left[ 1 - \left\{ 1 - \frac{8 \propto \frac{S}{K_s}}{\left(1 + \frac{S}{K_s} + \propto\right)^2} \right\}^{1/2} \right]$ | (Annuar et al., 2008) |
| 14. | Heijnen and Romein | $\mu = \mu_{max} \left[ \frac{\frac{S}{K_s}}{\frac{S}{K_s} - 1 + 2^{1/n}} \right]^n$ | (Annuar et al., 2008) |
| 15. | Aiba-Edwards | $\mu = \mu_{max} \frac{S}{K_s + S} e^{-S/K_i}$ | (González-figueredo et al., 2018; Halmi et al., 2014; Xu et al., 2018) |
| 16. | Webb | $\mu = \frac{\mu_{max} S \left(1 + \frac{S}{K_i}\right)}{S + K_s + \frac{S^2}{K_i}}$ | (Annuar et al., 2008; Tazdait et al., 2013) |
| 17. | Luong | $\mu = \frac{\mu_{max} S}{K_s + S} \left[ 1 - \frac{S}{S_m} \right]^n$ | (Abubakar et al., 2017; Shukor & Shukor, 2014; Xu et al., 2018) |
| 18. | Yano and Koga I | $\mu = \mu_{max} \left( \frac{S}{K_s + S + \frac{S^2}{K_1} + \frac{S^3}{K_2^2}} \right)$ | (Tazdait et al., 2013) |

**International Journal of Research in Science & Engineering**
**ISSN: 2394-8299**
Vol: 01, No. 02, Oct-Nov 2021
http://journal.hmjournals.com/index.php/IJRISE
**DOI:** https://doi.org/10.55529/ijrise.12.1.24

| | | | |
|---|---|---|---|
| 19. | Yano and Koga II | $\mu = \mu_{max}\left(\frac{S}{K_s + S + \frac{S^3}{K_2^2}}\right)$ | (Gummadi & Santhosh, 2010) |
| 20. | Han and Levenspiel | $\mu = \mu_{max} S\left[\frac{\left(1-\frac{S}{S_m}\right)^n}{S + K_s\left(1-\frac{S}{S_m}\right)^m}\right]$ | (Muloiwa et al., 2020; Tazdait et al., 2013) |
| 21. | Wayman and Tseng | $\mu = \frac{\mu_{max} S}{K_s + S} - i(S - S_\theta)$ | (Gummadi & Santhosh, 2010; Hamitouche et al., 2012; Shukor & Shukor, 2014) |
| 22. | Alagappan and Cowan | $\mu = \frac{\mu_{max} S}{K_s + S + \frac{S^2}{K_i}} - i(S - S_\theta)$ | (Hamitouche et al., 2012; Shukor & Shukor, 2014) |
| 23. | Double exponential | $\mu = \mu_{max}\left[e^{-S/K_i} - e^{-S/K_s}\right]$ | (Gummadi & Santhosh, 2010) |
| 24. | Logarithmic | $\mu = a + b_b \ln(S)$ | (Muloiwa et al., 2020) |
| 25. | Hinshelwood | $\mu = \frac{\mu_{max} S}{K_s + S}(1 - KP)$ | (Shariful Islam et al., 2021; Shukor & Shukor, 2014) |
| 26. | Proposed Model | $\mu = \frac{\mu_{max} S}{K_s + S + \frac{S^2}{K}}(1 - KP)$ | (Shariful Islam et al., 2021) |

where, $\mu_{max}$ = maximum specific growth rate ($hr^{-1}$), $K_s$ = saturation constant (mg/L), S = substrate concentration (mg/L), $S_m$ = terminal or maximum substrate inhibitory concentration at which growth stops or no growth is observed (mg/L), $K_i$, $K_1$ and $K_2$ = inhibition constant (mg/L), n = shape factor – constants which accounts for the relationship between μ and S, b = death constant ($hr^{-1}$), $X_m$ = maximum biomass concentration (mg/L), μ = specific growth rate ($hr^{-1}$), i = inhibition coefficient, m = curve parameter, ∝, a & $b_b$ are constants, and $S_\theta$ = threshold substrate concentration below which no inhibition is obvious (mg/L). Two other models that incorporate product concentration (P) are Hinshelwood and the Proposed model, where K = curve parameter as given in Table 1. Normally, before feeding CM to a biofermenter, analysis are usually carried out to determine the total solid, volatile solid, moisture content, nutrient content, ash content, particle density, carbon-to-nitrogen ratio and protein content among others (Abubakar & Yunus, 2021).

**International Journal of Research in Science & Engineering**
**ISSN: 2394-8299**
Vol: 01, No. 02, Oct-Nov 2021
http://journal.hmjournals.com/index.php/IJRISE
**DOI:** https://doi.org/10.55529/ijrise.12.1.24

### 2.2. Monod Equation

The simplest among the models is the Monod equation (Beltrán-prieto & Nguyen, 2018) for acidogenic bacteria kinetics. The classical equation describes the proportional link between the μ and low S, in turn explaining the microbial growth, physiology, and biochemistry (González-figueredo et al., 2018). The Monod model assumes that the digesting culture media has only one limiting substrate (González-figueredo et al., 2018; UlukardeŞler & Atalay, 2018). Two special cases for the Monod growth formulae exist: at high substrate concentration (i.e. $S \gg K_s$ with zero order), growth will occur at the maximal growth rate, $\mu_{max}$ while at low substrate concentration (i.e. $S \ll K_s$), growth will have a first order dependence on substrate concentration, as μ is highly sensitive to S. To determine the Monod constant parameters, a plot of μ againsts S obtained from experiments is done, where the substrate-affinity constant, $K_s$, which is the value of S at $\mu_{max}/2$ and $\mu_{max}$ which is the tangent to the inflection point is determined (Arifan et al., 2021). Alternatively, a straight line Lineweaver-Burke plot can be made when the reciprocal of the Monod equation is taken, thereby allowing the Monod equation to be transformed into an equation of a straight line with known slope and intercept, to help determine $\mu_{max}$ and $K_s$. Apart from this, the Eadie-Hofstee, Hanes-Woolf and the Integration equation, derived from the generic Monod equation can be exploited. Globally, it is agreed that the Monod model suffers some drawbacks. These limitations are (González-figueredo et al., 2018; Muloiwa et al., 2020): (a) Monod model not being able to describe specific growth rate in the presence of toxic substrate concentration or substrate inhibition effect, (b) separate entity, regulatory complex, adaptive sensitivity to environmental changes, and ability of cell organelles to produce various products in inherent metabolism cannot be considered, (c) at high S, the $\mu_{max}$ is independent of the substrate concentration, (d) at low S, growth is dependent on substrate concentration, (e) Monod model does not account for the fact that cells may require substrate for maintenance during the death phase and, (f) model does not account for the lag and death phase during the growth phase. To alleviate these disadvantages, without discarding its advantage, other models incorporating several other parameters have been developed.

### 2.3. Contois and Other Proposed Models

One important feature of the Contois model (Bayen et al., 2018) is that, cell mass growth rate depends on both substrate and cell concentrations with growth being inhibited at high concentration of microbes. The assumption here is that X is inversely proportional to μ (Muloiwa et al., 2020). It further explains the changes in population density that is of effect to the net specific growth rate through insertion of the biomass concentration, X, into the existing Monod structure (Annuar et al., 2008). The model had been used to examine the hydrolysis rate of extracellular enzymes in the course of production of a biochemical reaction by hydrolytic bacteria (Hassan et al., 2017). Just like the Monod model, Blackman model, and Tessier model, the Contois model cannot describe the lag and death phase and does not capture substrate inhibition (Muloiwa et al., 2020). The Andrews' equation for substrate inhibition is simple and widely accepted for describing growth inhibition kinetics of microorganisms (Tazdait et al., 2013). The same author went on to explain the inhibition constant. The inhibition constant, $K_i$ in Andrews' model describes the degree of toxicity of the substrate towards the bacterial population. Low $K_i$, shows the high sensitivity the microorganism had to

**International Journal of Research in Science & Engineering**
**ISSN: 2394-8299**
Vol: 01, No. 02, Oct-Nov 2021
http://journal.hmjournals.com/index.php/IJRISE
**DOI:** https://doi.org/10.55529/ijrise.12.1.24

substrate inhibition. Therefore, $K_i$ is the S at which bacterial growth or substrate degradation reduced to 50% of $\mu_{max}$ or maximum specific degradation rate of the substrate as a result of substrate inhibition. Another extension of the Monod equation is the unstructured and inhibitory model called Aiba-Edwards model. Aiba-Edwards model (González-figueredo et al., 2018) introduces an exponential to the ratio of S and inhibitory constant, $K_i$, a parameter that takes care of the presence of toxic S in the bioreactor. The model is capable of describing the lag and death phase but struggles when describing critical values of inhibitory substrate (Muloiwa et al., 2020). Halden model (Hamitouche et al., 2012) is an extended form of the Monod model by introducing the inhibition constant, $K_i$ at low and high substrate concentration, making the model being able to handle both toxic and non-toxic substrate (Delgadillo-Mirquez et al., 2018). It is also called the methanogenic microorganism kinetics used to emphasize the volatile fatty acid (VFA) accumulation causing inhibition in AD process (Delgadillo-Mirquez et al., 2018). Webb model is a modified version of the Haldane model, describing μ as a function of S only. Though, Webb's model intended to improve upon the Haldane model, an endeavour that wasn't successful (Muloiwa et al., 2020). Heijnen and Romein in 1995 both came up with a universal microbial growth and substrate uptake model by simplifying cellular procedures to a coupled scheme of anabolic and catabolic reactions (Annuar et al., 2008). Luong model can also be used to describe the kinetics of substrate inhibition. It allows the description of substrate limitation observed at a low concentration and also allow substrate inhibition observe at high concentration to be accounted for, through the parameter $S_m$ – the maximum substrate concentration above which growth ceases (Hamitouche et al., 2012; Xu et al., 2018). Moser model integrated a tunable parameter 'n' into the Monod framework, so as to account for potential interactions between binding sites on the enzyme molecule (Annuar et al., 2008; Muloiwa et al., 2020). Tessier model simply labels μ as an exponential function of the S, $\mu_{max}$, and $K_S$ (Annuar et al., 2008; Muloiwa et al., 2020). Blackman model had similar assumptions as the Monod model. At low S, growth is dependent on substrate and at high S, when nutrients is limiting, growth is independent of substrate concentration (Muloiwa et al., 2020). There is a first order relationship between μ and S at low S and a zero order relationship at higher S (Annuar et al., 2008). Yano and Koga suggested a model after a theoretical study on the dynamic performance of single-vessel continuous digestion subject to growth inhibition at high concentrations of rate-limiting substrates (Tazdait et al., 2013). Powell looks at the influence of passive diffusion of a particular substrate as the key limiting step affecting bacterial growth, without considering substrate inhibition, hence struggles to describe the lag and death phase (Annuar et al., 2008; Muloiwa et al., 2020).

The worst model due to its weakness in describing the lag, stationary, and death phase is agreed to be the Logarithmic model. Logarithmic model is well known for overestimating cell growth, and if the S is low, it can produce negative growth rate (Muloiwa et al., 2020). As clearly seen in Table 1, the model describes μ as a function of logarithm of S. Dabes derived a "3-parameter" model describing bacterial growth on a single limiting substrate by considering that only 2 of the long series of catalysed, reversible enzyme-substrate reactions involved in substrate metabolism had slow reaction rates (Annuar et al., 2008). Apart from those models mentioned in Table 1, other models exist as well. Schnute model is another growth model described by free parameters, each contributing to the characteristics of the curve: an initial lag phase, exponential growth phase, and reduced growth rate (Beltrán-prieto & Nguyen, 2018; Gummadi

**International Journal of Research in Science & Engineering**
**ISSN: 2394-8299**
Vol: 01, No. 02, Oct-Nov 2021
http://journal.hmjournals.com/index.php/IJRISE
**DOI:** https://doi.org/10.55529/ijrise.12.1.24

& Santhosh, 2010; Kyurkchiev et al., 2016). Applications are in population dynamics, population ecology, plant biology, bacterial growth, chemistry and statistics (Kyurkchiev et al., 2016). The Weibull model (Lobacz et al., 2020) and the Baranyi model (Hawkins et al., 2019; Kang et al., 2021) differs in terms of the chosen parameters. Baranyi model assumes that the course of the growth is influenced by the initial microbial cell concentration and the physiological state of the inoculum (Lobacz et al., 2020).

## 3. METHODOLOGY

### 3.1. Feedstock Preparation

CM sourced from the Faculty of Agriculture poultry farm of the University of Maiduguri was collected. The CM contains chicken dung, blood, urine, feather, and poultry feeds. Semi-solid CM sample weighing 7.2kg was collected and mixed with equal weight of water ($H_2O$) before it was fed into the digester shown in Fig. 1.

### 3.2. Determination of Cell Concentration

For 40 days, 5ml of CM slurry was drawn from the digester in Fig. 2, put in a 10ml white transparent bottle and taken to a Microbiological laboratory for microbial count. Each day, nine test tubes were washed clean and dried and 9ml of distilled $H_2O$ was poured inside all the tubes arranged in a rack, forming a single line. Using a 5ml syringe, 1ml of sample was drawn from the inoculum bottle and injected into the first tube in the row and shaked to mix properly. A procedure known as serial dilution that involves the continues transfer of 1ml from successive tubes up to the last tube was carried. It is recommended to mix the tube thoroughly after each transfer. Swe Biotech nutrient agar (NA) was prepared according to the instruction manual and allowed to cool to about 43℃. Three colony plates labelled 1, 2, and 3 were lined up and 1ml of diluted culture from tube 7, 8 and 9 was drawn and injected on plate 1, 2 and 3 respectively. The prepared NA was poured on the plates to cover its entire base and closed. The three plates are then incubated at 37℃ for 24 hours and withdrawn to be counted using a colony counter. This step was repeated on daily basis. Also note that before sample collection from the digester, the CM slurry is mixed for 3 minutes to ensure uniform composition. The whole procedure is illustrated in Fig. 3 and was carried out based on explanations given by Reynolds (2016), Sieuwerts et al. (2008) and Sanders (2012).

At the end of the experiment, the average of the counted colonies for the 3 tubes was recorded. Care was taken while carrying out this experiment as Ben-David & Davidson (2014) emphasized that sampling error and counting error could affect the count. Concentration of bacteria or cell (X) was presented in colony forming units (CFU) per millilitre based on Eq. 1 according to Arana et al. (2013) and Um-e-Habiba et al. (2021) using a total dilution factor (TDF) of $10^9$ for the average number of colonies computed.

$$\mathrm{CFU/mL} = \frac{(\text{No. of colonies})(\text{TDF})}{\text{Volume of culture plated in ml}} \qquad (1)$$

Assuming a single cell weighing around 1ng grows to form a single colony or 1 CFU/mL, X data earlier recorded in CFU/mL units was converted to mg/L.

**International Journal of Research in Science & Engineering**
**ISSN: 2394-8299**
Vol: 01, No. 02, Oct-Nov 2021
http://journal.hmjournals.com/index.php/IJRISE
**DOI:** https://doi.org/10.55529/ijrise.12.1.24

Fig. 1. CM Slurry Fed to an Anaerobic Digester

**(a)** – Collected CM Sample; **(b)** – CM plus water; **(c) –** Injected CM Feedstock; **(d)** – Complete Digester Setup

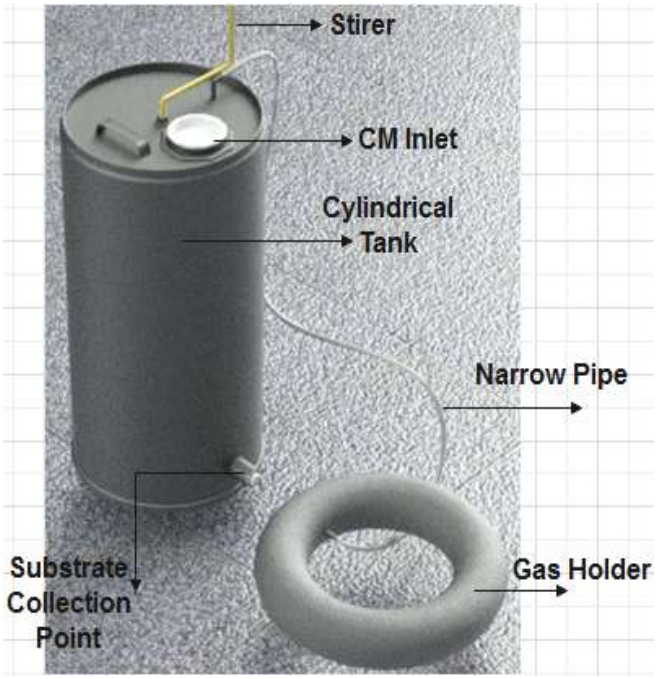


Fig. 2**.** Bioreactor with Gas Collector

**International Journal of Research in Science & Engineering**
**ISSN: 2394-8299**
Vol: 01, No. 02, Oct-Nov 2021
http://journal.hmjournals.com/index.php/IJRISE
**DOI:** https://doi.org/10.55529/ijrise.12.1.24

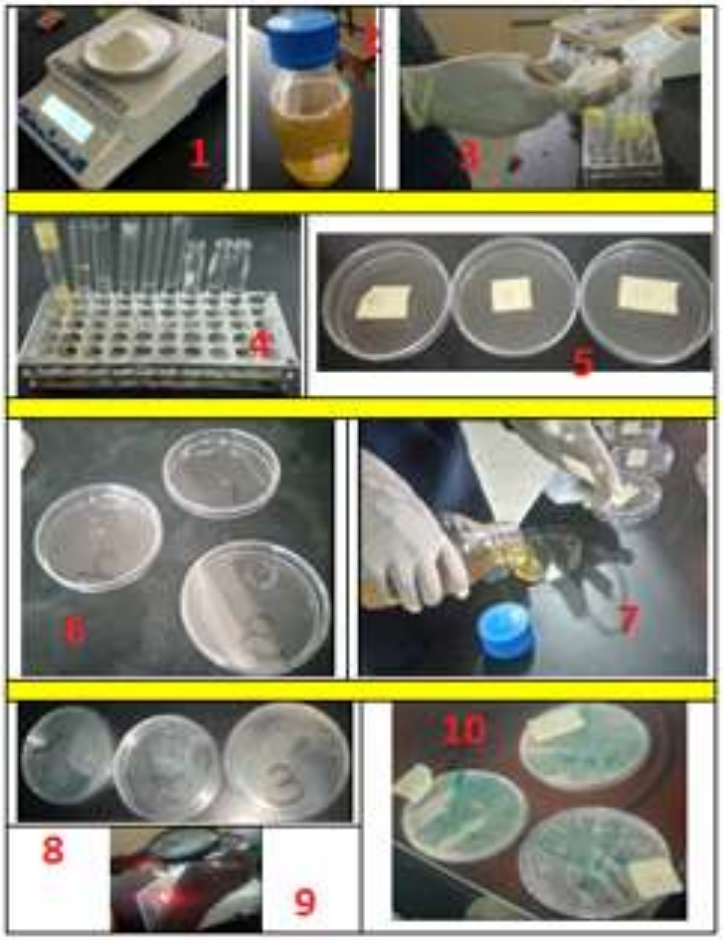


Fig. 3. Experimental Steps of Cell Count:

**1** – NA measurement; **2** – Prepared liquid NA; **3 –** CM slurry as inoculum; **4** – Tubes after serial dilution; **5** – Labelled plates; **6** – Plates with 1mL of dilution; **7 –** Pour plating; **8** – Plates after incubation; **9** – Electronic colony counter; **10** – Visible colonies on plates.

### 3.3. Estimation of Substrate Concentration

Firstly, initial substrate concentration ($S_0$) was determined by dividing the total amount of CM fed in the digester by the amount of $H_2O$ added at the beginning of the work, kept in mg/L units. Subsequent substrate concentration (S) or S empirical ($S_{Emp.}$) that is depleting with time in the digester was estimated using Eq. 2 after assuming a biomass-to-substrate yield coefficient, Y of 400 using their initial ratio.

$$S_{Emp.} = S_o - \frac{X_{Emp.} - X_o}{Y} \qquad (2)$$

Where, $X_{Emp.}$ is the X (mg/L) computed from experimental steps.

### 3.4. Monod Parameter Estimation

From Monod model given by Eq. 3 (Dlangamandla et al., 2019),

**International Journal of Research in Science & Engineering**
**ISSN: 2394-8299**
Vol: 01, No. 02, Oct-Nov 2021
http://journal.hmjournals.com/index.php/IJRISE
**DOI:** https://doi.org/10.55529/ijrise.12.1.24

$$\mu = \frac{\mu_{max}\, S}{K_s + S} \qquad (3)$$

parameters such as the maximum specific growth rate, $\mu_{max}$ (mg of new cells/mg of cells/day), and half-saturation constant, $K_s$ was estimated by finding appropriate substrate concentration data as well as the specific growth rate, μ. The Malthus equation of growth of the microorganisms present or Eq. 4 (Abubakar et al., 2017) was combined with Eq. 5, and integrated by making X subject.

$$\frac{dX}{dt} = \mu X \qquad (4)$$

$$\mu = k\left(1 - \frac{X}{X_\infty}\right) \qquad (5)$$

Where, t = retention time (day), $X_\infty$ = maximal biomass concentration = $X_0 + YS_0$ (mg/L) and k = maximum specific substrate utilization rate (g substrate/g of microorganism/day). This X is referred to as X correlated, (or $X_{Corr.}$) and is given by Eq. 6.

$$X_{corr.} = \frac{X_0 e^{kt}}{1 - \frac{X_0}{X_\infty}[1 - e^{kt}]} \qquad (6)$$

It was estimated using empirical S and X (or $X_{Emp.}$ and $S_{Emp.}$) over the 40 days retention time using POLYMATH 6.1 regression tool, so as to estimate the value of k at better fit. Corresponding, $S_{corr.}$ data was generated using Eq. 7, which is similar to Eq. 2 using the $X_{corr.}$ values.

$$S_{corr.} = S_o - \frac{X_{corr} - X_o}{Y} \qquad (7)$$

The parameter, $K_s$, was estimated by combining the Monod model with Eq. 5, making S the subject. Using $X_{corr.}$ values, regression was performed guessing different values of the unknown parameters in Eq. 8, where the estimated S from regression or $S_{reg}$ is approximately equal to $S_{corr.}$ results.

$$S_{reg} = \frac{K_s\left(\frac{X_\infty - X_{corr}}{X_\infty}\right)}{Y - \left(\frac{X_\infty - X_{corr}}{X_\infty}\right)} \qquad (8)$$

In Equation 3.8, the term, $\frac{\mu_{max}}{k}$, was obtained originally, but substituted with Y (Talaiekhozani et al., 2015). Rate of cell growth data was generated by combining Eq. 4 and Eq. 5, resulting in Eq. 9.

$$\frac{dX}{dt} = k\left(1 - \frac{X_{corr}}{X_\infty}\right) X_{corr} \qquad (9)$$

Using $\frac{dX}{dt}$ data, μ values were computed using Eq. 10 gotten after re-arranging Eq. 4.

$$\mu = \frac{1}{X_{corr}} \frac{dX}{dt} \qquad (10)$$

Eq. 11 was developed from the Monod kinetic model to calculate new set of S values called $S_{Monod}$.

$$S_{Monod} = \frac{\mu K_s}{\mu_{max} - \mu} \qquad (11)$$

**International Journal of Research in Science & Engineering**
**ISSN: 2394-8299**
Vol: 01, No. 02, Oct-Nov 2021
http://journal.hmjournals.com/index.php/IJRISE
**DOI:** https://doi.org/10.55529/ijrise.12.1.24

A plot of μ against $S_{Monod}$ was carried out to give the Monod plot where values of $K_s$ and $\mu_{max}$ that will be determined are deemed identical with ones obtained through regression with POLYMATH.

### 3.5. Growth Model Fitting to Measured Data

Unknown kinetic model parameters in growth models earlier listed in Table 1 was estimated applying the Levenberg-Marquardt nonlinear method of regression using POLYMATH by first estimating regression parameters such as the coefficient of determination ($R^2$), Root-Mean Square Error (RMSE), and adjusted $R^2$.

## 4. RESULTS

### 4.1. Cell and Substrate Concentration

Number of dilutions resulting in a certain dilution factor (DF) affects the resulting number of colonies visible to count. The higher the number of dilutions, the lower the number of microorganisms that will form visible colonies; while the lower the number of dilutions, the higher the microorganisms that would form colonies and hence form too numerous colonies. Datta (2021) reported TDF of $10^{14}$ for tap water microbial count, giving $36 \times 10^{16}$ CFU/ml while Luka et al. (2014) reported up to $0.7 \times 10^{12}$ CFU/l for Bacillus subtilis in wastewater. Here, it is clear that cells concentration increases after maintaining a constant density of $3.67 \times 10^6$ mg/l for 7 days called the lag phase, from $5.33 \times 10^6$ mg/l to $3.40 \times 10^8$ mg/l during a period referred to as the exponential growth phase. The lag phase is known as the acclimatization phase, where all the bacteria present starts to adopt to the CM environment they are kept in. Also, changes in microorganism population is very insignificant to effect any changes in the substrate level. After acclimatization, the increase witness at day 8, over a 23 days duration, signifies a healthy microbial growth due to sufficient nutrient available. Table 2 shows the CFU/ml of the hypothetical microorganism present in the CM.

Table 2. Substrate Concentration Calculated Based on Experimental Values of Cell Concentration

| Time (days) | X (CFU/mL) | X (Expt.) (mg/L) | S (Expt.) (mg/L) | Time (days) | X (CFU/mL) | X (Expt.) (mg/L) | S (Expt.) (mg/L) |
|---|---|---|---|---|---|---|---|
| 0 | 3666666667 | 3666666.667 | 952380.95 | 21 | 1.11E+11 | 111333000 | 683215.1167 |
| 1 | 3666666667 | 3666666.667 | 952380.95 | 22 | 1.20E+11 | 120000000 | 661547.6167 |
| 2 | 3666666667 | 3666666.667 | 952380.95 | 23 | 1.41E+11 | 141000000 | 609047.6167 |
| 3 | 3666666667 | 3666666.667 | 952380.95 | 24 | 1.61E+11 | 160667000 | 559880.1167 |

**International Journal of Research in Science & Engineering**
**ISSN: 2394-8299**
Vol: 01, No. 02, Oct-Nov 2021
http://journal.hmjournals.com/index.php/IJRISE
**DOI:** https://doi.org/10.55529/ijrise.12.1.24

| | | | | | | | |
|---|---|---|---|---|---|---|---|
| 4 | 3666666667 | 3666666.667 | 952380.95 | 25 | 1.77E+11 | 176667000 | 519880.1167 |
| 5 | 3666666667 | 3666666.667 | 952380.95 | 26 | 1.92E+11 | 192000000 | 481547.6167 |
| 6 | 3666666667 | 3666666.667 | 952380.95 | 27 | 2.36E+11 | 236000000 | 371547.6167 |
| 7 | 3666666667 | 3666666.667 | 952380.95 | 28 | 2.55E+11 | 255333000 | 323215.1167 |
| 8 | 5333333333 | 5333333.333 | 948214.2833 | 29 | 2.81E+11 | 280667000 | 259880.1167 |
| 9 | 9000000000 | 9000000 | 939047.6167 | 30 | 3.40E+11 | 339667000 | 112380.1167 |
| 10 | 12333333333 | 12333333.33 | 930714.2833 | 31 | 3.41E+11 | 341000000 | 109047.6167 |
| 11 | 18333333333 | 18333333.33 | 915714.2833 | 32 | 3.39E+11 | 339000000 | 114047.6167 |
| 12 | 23000000000 | 23000000 | 904047.6167 | 33 | 3.33E+11 | 333333000 | 128215.1167 |
| 13 | 30666666667 | 30666666.67 | 884880.95 | 34 | 3.39E+11 | 339000000 | 114047.6167 |
| 14 | 40000000000 | 40000000 | 861547.6167 | 35 | 3.40E+11 | 339667000 | 112380.1167 |
| 15 | 52000000000 | 52000000 | 831547.6167 | 36 | 3.43E+11 | 343000000 | 104047.6167 |
| 16 | 57666666667 | 57666666.67 | 817380.95 | 37 | 3.34E+11 | 334000000 | 126547.6167 |
| 17 | 69333333333 | 69333333.33 | 788214.2833 | 38 | 2.56E+11 | 256000000 | 321547.6167 |
| 18 | 72666666667 | 72666666.67 | 779880.95 | 39 | 1.79E+11 | 179000000 | 514047.6167 |
| 19 | 88666666667 | 88666666.67 | 739880.95 | 40 | 1.40E+11 | 140000000 | 611547.6167 |
| 20 | 1.03E+11 | 102667000 | 704880.1167 | | | | |

At day 31-37, the population is almost constant. This is because the rate at which new cells are formed equals the rate at which cells die, and is known as the stationary phase. The death phase is witnessed after this period due to cell destruction or the accumulation of toxic substances. It is therefore clear that as substrate concentration decreases, the population of microorganism increase and vice versa.

### 4.2 Monod Parameters

When S is low or $S \ll K_s$, growth is said to have a first order dependence on S whereas when it is high or $S \gg K_s$, growth is at $\mu_{max}$ and growth will have a zero-order dependence on S.

**International Journal of Research in Science & Engineering**
**ISSN: 2394-8299**
Vol: 01, No. 02, Oct-Nov 2021
http://journal.hmjournals.com/index.php/IJRISE
**DOI:** https://doi.org/10.55529/ijrise.12.1.24

Fig. 4 illustrate this by dividing the Monod plot into three regions. The middle section satisfies the Monod expression, while the extreme regions modifies Equation 3 based on the behaviour of S

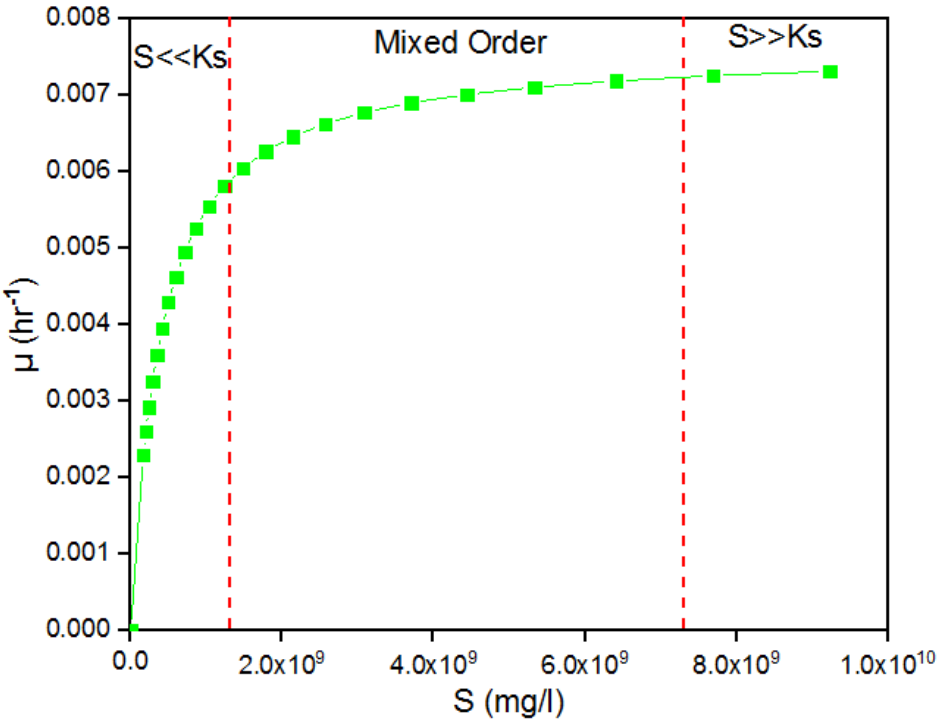


Fig. 4. Specific Growth Rate versus Substrate Concentration.

### 4.3. Microbial Growth Kinetic Model Fitting

In this work, 24 growth kinetic models identified in the literature was fitted to empirical data so as to estimate their respective kinetic parameters. The fitted plots are shown in Fig. 6-12, where 5 models including Monod with decay rate, Wayman & Tseng, Han & Levenspiel, Luong and Moser models had $R^2 = 1$, which imply that all the points lie on the regression line (with no errors). RMSE's of these models are closer to 0, also indicating a good fit with same estimates ($\mu_{max} = 0.0076201 h^{-1}$ & $K_s = 3.838 \times 10^8$ mg/l) compared to Monod parameters. Coefficient of determination, $R^2 = 0.999777$ in Webb model is 99.98% fitted to the Monod line, though type of parameters estimated are not the same in all the 6 models so far mentioned.

If models are to be compared based on unique parameters estimated, then Monod with decay rate (with estimated parameters: $\mu_{max}$, $K_s$, $K_i$ & b), Wayman and Tseng (with estimated parameters: $\mu_{max}$, $K_s$, i, $K_i$ & $S_\theta$), Webb (with estimated parameters: $\mu_{max}$, $K_s$ & $K_i$) and Luong (with estimated parameters: $\mu_{max}$, $K_s$, n, m & $S_m$) are models that fits perfectly to Monod plot or experimental data obtained in this work. Models such as Double exponential, Haldane, Aiba-Edwards, Andrew, Halden, Andrew with decay rate and Webb model estimated the same inhibition constant, $K_i = 1.01 \times 10^{12}$ except for Alagappan and Cowan where $K_i = -2.643 \times 10^8$. Alagappan and Cowan model, otherwise called the modified Wayman and Tseng model, can be said to be the worst model as none of the estimated parameters is positive

**International Journal of Research in Science & Engineering**
**ISSN: 2394-8299**
Vol: 01, No. 02, Oct-Nov 2021
http://journal.hmjournals.com/index.php/IJRISE
**DOI:** https://doi.org/10.55529/ijrise.12.1.24

and shows a deviating curve in Fig. 6. Han and Levenspiel and Luong models are the only two models with maximum substrate concentration, $S_m$, presenting a 100% fit (see Fig. 11 and Table 3).

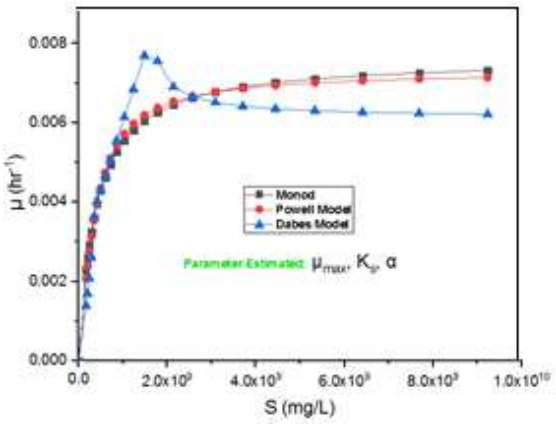


Fig. 5. Fitting Powel and Dabes Model to Monod Plot

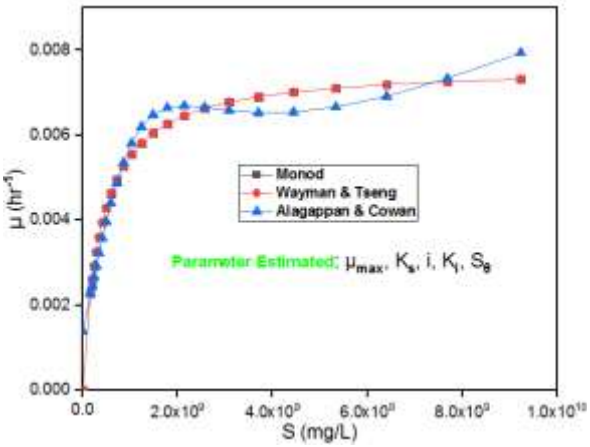


Fig. 6. Fitting (i) Wayman & Tseng and (ii) Alagappan & Cowan Model to Monod Equation

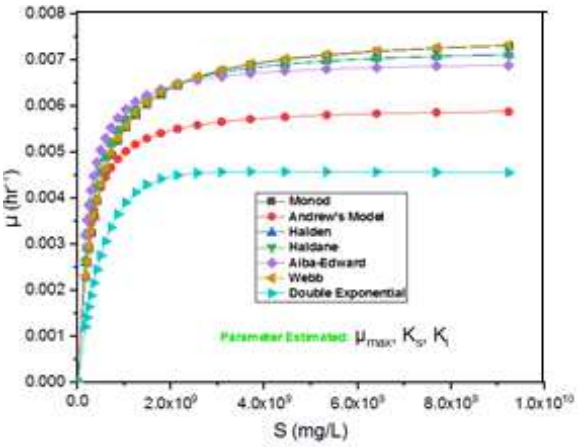


Fig. 7. Estimating $\mu_{max}$, $K_s$ & $K_i$ by Fitting Six Growth Models to Monod Data

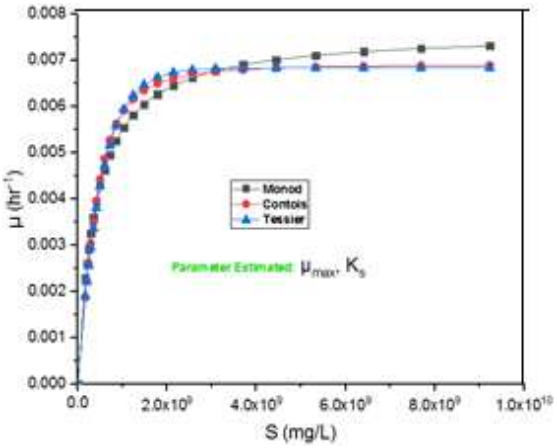


Fig. 8. Contois and Tessier Model Parameter Estimation by Regression

**International Journal of Research in Science & Engineering**
**ISSN: 2394-8299**
Vol: 01, No. 02, Oct-Nov 2021
http://journal.hmjournals.com/index.php/IJRISE
**DOI:** https://doi.org/10.55529/ijrise.12.1.24

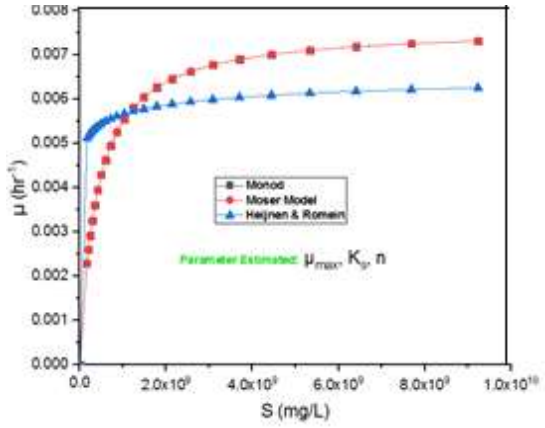


Fig. 9. Estimating Growth Parameters by Data Fit using Monod

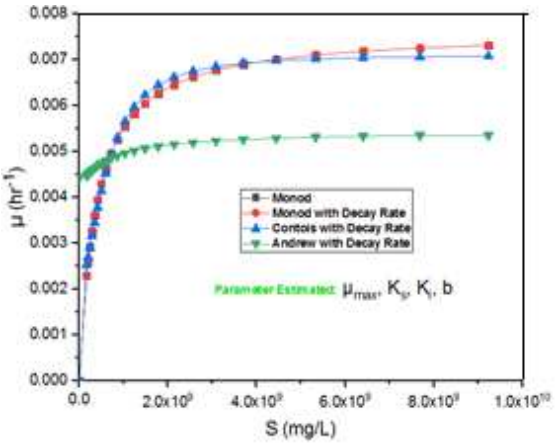


Fig. 10. Monod Fitted to Models Based on Substrate Decay Rate

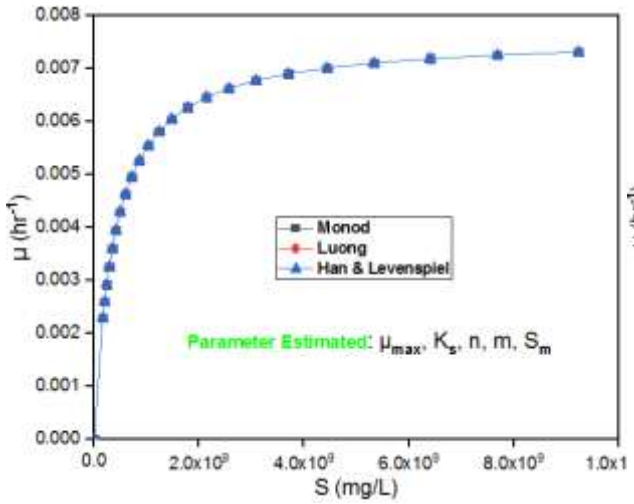


Fig. 11. Luong and Han & Levenspiel Microbial Growth Parameter Estimate by Regression with Monod Equation

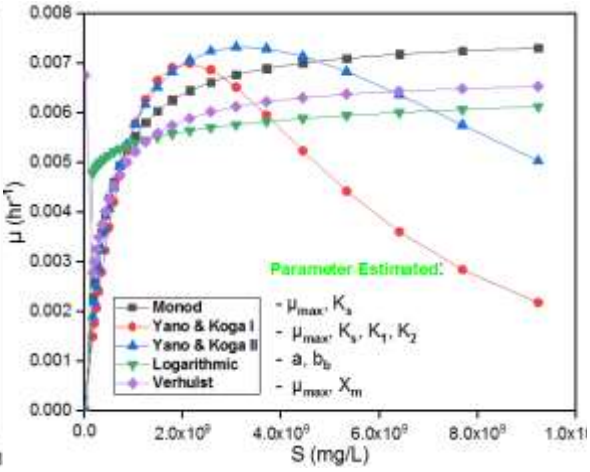


Fig. 12. Verhulst, Logarithmic and Yano & Koga I and II Estimates of Growth Parameters from Monod Data μ

Table 3. Growth Kinetics and Statistical Parameter Estimates from POLYMATH

| Model | Parameter | $R^2$ | Adj. $R^2$ | RMSE | Model | Parameter | $R^2$ | Adj. $R^2$ | RMSE |
|---|---|---|---|---|---|---|---|---|---|
| Monod | $\mu_{max} = 0.007620$ $K_s = 3.838 \times 10^8$ | 1.0000 | 1.0000 | 1.05E-06 | Andrew with Decay rate | $\mu_{max} = 0.001224$ $K_s = 8.621 \times 10^8$ $K_i = 1.01 \times 10^{12}$ | 0.474 | 0.39568 | 0.006745 |

**International Journal of Research in Science & Engineering**
**ISSN: 2394-8299**
Vol: 01, No. 02, Oct-Nov 2021
http://journal.hmjournals.com/index.php/IJRISE
**DOI:** https://doi.org/10.55529/ijrise.12.1.24

| | | | | | | | | | |
|---|---|---|---|---|---|---|---|---|---|
| | | | | | | $b = -0.0042$ | | | |
| Monod with Decay rate | $\mu_{max} = 0.00762($ $K_s = 3.838 \times 10^{8}$ $b = -8.207 \times 10^{-8}$ | 1.00 00 | 1.00 00 | 1.05 E-06 | Moser | $\mu_{max} = 0.00762($ $K_s = 3.838 \times 10^{8}$ $n = 0.99999$ | 1.0 00 | 1.0000 | 1.18E -05 |
| Contois | $\mu_{max} = 0.00691$ $K_s = 1.64995$ | 0.98 033 | 0.97 944 | 0.00 12 | Tessier | $\mu_{max} = 0.00683$ $K_s = 5.061 \times 10^{8}$ | 0.9 76 | 0.9745 8 | 0.001 287 |
| Contois with Decay rate | $\mu_{max} = 0.00535$ $K_s = 3.68492$ $b = -0.0017$ | 0.99 502 | 0.99 456 | 0.00 06 | Halden | $\mu_{max} = 0.00742$ $K_s = 3.063 \times 10^{8}$ $K_i = 1.01 \times 10^{12}$ | 0.9 88 | 0.9867 7 | 0.000 868 |
| Andrew | $\mu_{max} = 0.00607$ $K_s = 2.142 \times 10^{8}$ $K_i = 1.01 \times 10^{12}$ | 0.39 251 | 0.33 465 | 0.00 33 | Haldan e | $\mu_{max} = 0.00741$ $K_s = 3.035 \times 10^{8}$ $K_i = 1.01 \times 10^{12}$ | 0.9 87 | 0.9858 9 | 0.000 899 |
| Verhuls t | $\mu_{max} = 0.00676$ $X_m = 4.566 \times 10^{8}$ | 0.41 148 | 0.38 474 | 0.00 35 | Dabes | $\mu_{max} = 0.00311($ $K_s = 3.187 \times 10^{8}$ $\alpha = 1.40275$ | 0.8 48 | 0.8337 0 | 0.002 885 |
| Powell | $\mu_{max} = 0.00545$ $K_s = 2.301 \times 10^{8}$ | 0.99 557 | 0.99 515 | 0.00 05 | Heijne n and Romei n | $\mu_{max} = 0.00655$ $K_s = 8.411 \times 10^{4}$ | 0.5 53 | 0.5105 374 | 0.005 043 |

**International Journal of Research in Science & Engineering**
**ISSN: 2394-8299**
Vol: 01, No. 02, Oct-Nov 2021
http://journal.hmjournals.com/index.php/IJRISE
**DOI:** https://doi.org/10.55529/ijrise.12.1.24

| | | | | | | | | | |
|---|---|---|---|---|---|---|---|---|---|
| | $\alpha = 1.158878$ | | | | | $n = 0.058796$ | | | |
| Aiba-Edwards | $\mu_{max} = 0.007104$ $K_s = 2.013 \times 10^8$ $K_i = 1.01 \times 10^{12}$ | 0.91568 | 0.90766 | 0.0022 | Yano and Koga I | $\mu_{max} = 0.015321$ $K_s = 1.521 \times 10^9$ $K_1 = 1.01 \times 10^{10}$ $K_2 = 4.157 \times 10^9$ | 0.135 | 0.0053872 | 0.005634 |
| Webb | $\mu_{max} = 0.007604$ $K_s = 3.764 \times 10^8$ $K_i = 1.01 \times 10^{12}$ | 0.99977 | 0.99976 | 0.0001 | Han and Levenspiel | $\mu_{max} = 0.007610$ $K_s = 3.833 \times 10^8$ $S_m = 4.57 \times 10^{11}$ $n = -0.0003$ $m = 1.532309$ | 1.000 | 1.0000 | 8.53E-08 |
| Luong | $\mu_{max} = 0.007620$ $K_s = 3.838 \times 10^8$ $S_m = 1.01 \times 10^{12}$ $n = -0.0003$ | 1.0000 | 1.000 | 2.44E-08 | Alagappan and Cowan | $\mu_{max} = -0.0482$ $K_s = -9.9 \times 10^9$ $K_i = -2.643 \times 10^8$ $i = -5.61 \times 10^{-13}$ $S_\theta = -2.452 \times 10^9$ | 0.952 | 0.9421286 | 0.001577 |
| Wayman and Tseng | $\mu_{max} = 0.007620$ | 1.0000 | 1.000 | 1.356E-09 | Double exponential | $\mu_{max} = 0.004602$ | 0.033 | -0.058988 | 0.008705 |

**International Journal of Research in Science & Engineering**
**ISSN: 2394-8299**
Vol: 01, No. 02, Oct-Nov 2021
http://journal.hmjournals.com/index.php/IJRISE
**DOI:** https://doi.org/10.55529/ijrise.12.1.24

| | | | | | | | | | |
|---|---|---|---|---|---|---|---|---|---|
| | $K_s = 3.838 \times 10^8$ $S_\theta = 8.276 \times 10^8$ i $= -1.67 \times 10^{-20}$ | | | | | $K_i = 1.01 \times 10^{12}$ $K_s = 5.407 \times 10^8$ | | | |
| Logarithmic | a $= -0.0015$ $b_b = 0.00033$ | 0.58252 | 0.56355 | 0.00053 | Yano and Koga II | $\mu_{max} = 0.00960$ $K_s = 6.698 \times 10^8$ $K_2 = 1.01 \times 10^{10}$ | 0.874 | 0.8623 | 0.000677 |

In the literature, Haldane model was found to be the best model to fit the growth kinetic data of Bacillus sp. grown in a medium containing chromium, as reported by Halmi et al. (2014). Luong is the most suitable kinetic model while modelling Tributyltin (TBT) in cadmium media as stated by Abubakar et al. (2017). While Shukor & Shukor (2014) stated that Han and Levenspiel is better compared to Luong in fitting the reduction of kinetic data. In the analysis carried out by UlukardeŞler and Atalay (2018b), application of Contois equation with decay rate for CM gave $\mu_{max} = 0.3$ and b = 0.5 for CM having dry solid (%) of 26.975. Growth of microorganisms in CM is rarely studied, hence there is few available data on parameters estimated to compare values obtained here. However, where a near 100% fit is witnessed, it would mean that the assumptions made leading to the development of such models works perfectly well for the CM substrate digested.

**Recap**

Biogas discovery has solved challenges faced in recent times where they are maximally utilized, such as pollution problems caused by indiscriminate dumping of animal residues, agricultural byproducts, and wastewaters from homes and industries. The chief facilitators of biogas production of these organic waste in order to arrest the environmental concerns they pose are microorganism, which are in turn harmful to humans exploiting them. In an oxygen-free environment some of these organisms digest these waste products to biogas at their survival temperature. CM is known to have naturally, some microorganisms including Bacillus cereus, Staphylococcus epidermis, Escherichia coli and Staphylococcus aureus (Adegunloye, 2006; Nodar et al., 1990). Scientist had studied the stages and factors influencing their survival during such processes up to the extent of developing model equations to explain their responses/rate of substrate conversion to biogas. Twenty of these models are identified and was used to fit observed results.

**International Journal of Research in Science & Engineering**
**ISSN: 2394-8299**
Vol: 01, No. 02, Oct-Nov 2021
http://journal.hmjournals.com/index.php/IJRISE
**DOI:** https://doi.org/10.55529/ijrise.12.1.24

Among them, Monod equation is the simplest and explains the bacterial affinity for nutrients in the CM waste feedstock. After a successful combination of the exponential growth equations (or Equation 4) and Equation 3, which is the Monod equation, a plot of μ against S better explains this affinity in three different cases/amount of substrate present, and helps determine both $K_s$ and $\mu_{max}$. Alternatively, instead of the usual Monod plots to estimate this parameters, other scientist/researchers had used the Lineweaver-Burke plot, Eadie-Hofstee plot and the Hanes-Woolf plot (Johnson, 2013). Apart from the Contois and Andrew's models of microbial analysis, the remaining models are least studied. In the literature, such models are hardly used to analyse growth in a particular organic material, but are rather used to study growth of certain isolated microbial species. Hence, this work is novel, in that, it analysed the growth of microbes in CM in respective of the kind or type of microorganism present. The graphical fittings of Figure 5-12 shows positive relationship between μ and S in almost all of the models used. Some of the models fit empirical results while some deviates due to modifications in the equation's structure and kinetic parameters in their model, thereby giving lower or higher values of $R^2$, RMSE and adjusted $R^2$ as shown in Table 3.

## 6. CONCLUSION

For the first time, more than 20 existing growth models have been fitted to experimental results of a particular material (specifically CM). For the microorganism present in the CM feedstock used, best models are those with highest $R^2$ and adjusted $R^2$ and lowest RMSE values when fitted to the simple Monod equation. Comparison of these growth models to determine the most suitable/correct for such analysis is hereby recommended using softwares such as the Origin 2018 version 95E using regression parameters such as Akaike's Information Criteria (AIC), Bayesian Information Criterion (BIC), Accuracy Factor (AF), Bias Factor (BF), Mean Absolute Percentage Error (MAPE) and F-test. Models involving product concentration has not been analysed for CM in this work, as one of the drawbacks. Also, identification of the type of microorganism responsible for the degradation of the substrate is recommended.

**Acknowledgement**
Much appreciation goes to Prof. Dr. Cahit Pesen for allowing this work get presented in the 3rd International SIIRT Conference on Scientific Research-IKSAD Institute, Siirt University, Türkiye, between November, 18-19, 2022 by the corresponding author.

**Conflict of Interest**
There are no conflicts of interest declared by the authors.

## 7. REFERENCES

1. Abubakar, A. M., & Yunus, M. U. (2021). Reporting biogas data from various feedstock. International Journal of Formal Sciences: Current and Future Research Trends (IJFSCFRT), 11(1), 23–36. https://doi.org/10.5281/zenodo.6366775
2. Abubakar, A., Usman, N. I., Ibrahim, H., Sunusi, U., Mohamat-yusuff, F., & Ibrahim, S. (2017). Growth kinetics modelling of tributytin-resistant Klebsiella sp. FIRD 2 in

**International Journal of Research in Science & Engineering**
**ISSN: 2394-8299**
Vol: 01, No. 02, Oct-Nov 2021
http://journal.hmjournals.com/index.php/IJRISE
**DOI:** https://doi.org/10.55529/ijrise.12.1.24

cadmium media. UMYU Journal of Microbiology Research, 2(1), 157–165.

3. Abubakar, B. S. U., Abdullah, N., Idris, A., Zakaria, M. P., & Shokur, M. Y. (2017). Estimating the biodegradation kinetics by mixed culture degrading pyrene(pyr). In Arid Zone Journal of Engineering, Technology and Environment (Vol. 13, Issue 1). www.azojete.com.ng
4. Adegunloye, D. (2006). Microorganisms associated with poultry faeces. Journal of Food, Agriculture and Environment, 4, 41–42.
5. Annuar, M. S. M., Tan, I. K. P., Ibrahim, S., & Ramachandran, K. B. (2008). A kinetic model for growth and biosynthesis of medium-chain-length poly-(3-hydroxyalkanoates) in Pseudomonas pudita. Brazilian Journal of Chemical Engineering, 25(02), 217–228. www.abeq.org.br/bjche
6. Arana, I., Orruno, M., & Barcina, I. (2013). How to solve practical aspects of microbiology (pp. 1–10).
7. Arifan, F., Abdullah, A., & Sumardiono, S. (2021). Kinetic study of biogas production from animal manure and organic waste in Semarang City by using anaerobic digestion method. Indonesian Journal of Chemistry, 21(5), 1221–1230. https://doi.org/10.22146/ijc.65056
8. Bayen, T., Rapaport, A., & Tani, F. Z. (2018). Optimal periodic control of the chemostat with Contois growth function. IFAC International Conference on Mathematical Modelling-(MATHMOD 2018), 730–734. https://doi.org/10.1016/j.ifacol.2018.03.124
9. Beltrán-prieto, J. C., & Nguyen, L. H. N. S. (2018). Numerical analysis of initial amount of substrate and biomass in substrate inhibition process. WSEAS Transactions on Systems and Control, 13, 491–496.
10. Ben-david, A., & Davidson, C. E. (2014). Estimation method for serial dilution experiments. Journal of Microbiological Methods, 107, 214–221. https://doi.org/10.1016/j.mimet.2014.08.023
11. Chen, Z., & Jiang, X. (2014). Microbiological safety of chicken litter or chicken litter-based organic fertilizers: A review. Agriculture, 4, 1–29. https://doi.org/10.3390/agriculture4010001
12. Cho, S., Hiott, L. M., Barrett, J. B., Mcmillan, E. A., House, S. L., Humayoun, S. B., Adams, E. S., Jackson, C. R., & Frye, J. G. (2018). Prevalence and characterization of Escherichia coli isolated from the Upper Oconee Watershed in Northeast Georgia. PLOS ONE, 13(5), 1–15. https://doi.org/https://doi.org/10.1371/journal.pone.0197005
13. Datta, A. (2021). Determination of viable microbial count present in tap water. International Journal of Innovative Science and Research Technology, 6(4), 246–247. https://doi.org/10.1520/STP36000S.The
14. Delgadillo-Mirquez, L., Hernández-sarabia, M., & Machado-Higuera, M. (2018). Mathematical modelling and simulation for biogas production from organic waste. International Journal of Engineering Systems Modelling and Simulation, 10(2), 97–102.
15. Dlangamandla, N., Ntwampe, S. K. O., Angadam, J. O., Chidi, B. S., & Mewa-ngongang, M. (2019). Kinetic parameters of Saccharomyces cerevisiae alcohols production using Nepenthes mirabilis pod digestive fluids-mixed agro-waste

**International Journal of Research in Science & Engineering**
**ISSN: 2394-8299**
Vol: 01, No. 02, Oct-Nov 2021
http://journal.hmjournals.com/index.php/IJRISE
**DOI:** https://doi.org/10.55529/ijrise.12.1.24

hydrolysates. Fermentation, 5(10), 1–14. https://doi.org/10.3390/fermentation5010010
16. Elbing, K., & Brent, R. (2020). Recipes and tools for culture of Escherichia coli. HHS Public Access, 125(1), 1–19. https://doi.org/10.1002/cpmb.83.Recipes
17. González-figueredo, C., Flores-estrella, R. A., & Rojas-rejón, O. A. (2018). Fermentation: Metabolism, kinetic models, and bioprocessing. In Current Topics in Biochemical Engineering (pp. 1–17). InTech Open. https://doi.org/http://dx.doi.org/10.5772/intechopen.82195 solid
18. Gummadi, S. N., & Santhosh, D. (2010). Kinetics of growth and caffeine demethylase production of Pseudomonas sp. in bioreactor. Journal of Ind Microbiology Biotechnology, 37, 901–908. https://doi.org/10.1007/s10295-010-0737-2
19. Halmi, M. I. E., Shukor, M. S., Johari, W. L. W., & Shukor, M. Y. (2014). Mathematical modeling of the growth kinetics of Bacillus spp. on tannery effluent containing chromate. Journal of Environmental Bioremediation & Toxicology (JEBAT), 2(1), 6–10. http://journal.hibiscuspublisher.com
20. Hamitouche, A., Bendjama, Z., Amrane, A., Kaouah, F., & Hamane, D. (2012). Relevance of the Luong model to describe the biodegradation of phenol by mixed culture in a batch reactor. Ann Microbiology, 62, 581–586. https://doi.org/10.1007/s13213-011-0294-6
21. Hassan, M., Umar, M., Ding, W., & Mehryar, E. (2017). Methane enhancement through co-digestion of chicken manure and oxidative cleaved wheat straw: Stability performance and kinetic modeling perspectives. Energy, 141, 2314–2320. https://doi.org/https://doi.org/10.1016/j.energy.2017.11.110
22. Hawkins, J. L., Uknalis, J., Oscar, T. P., Schwarz, J. G., Vimini, B., & Parveen, S. (2019). The effect of previous life cycle phase on the growth kinetics, morphology, and antibiotic resistance of Salmonella Typhimurium DT104 in brain heart infusion and ground chicken extract. Frontiers in Microbiology, 10(1043), 1–11. https://doi.org/10.3389/fmicb.2019.01043
23. Hossain, M. F., Rahman, M. T., & Kabir, S. M. L. (2017). Microbial assessment of milk collected from different markets of Mymensingh, Gazipur and Sherpur districts of Bangladesh and determination of antimicrobial resistance patterns of the isolated bacteria. Asian-Australasian Journal of Food Safety and Security, 1(1), 7–16. www.ebupress.com/journal/aajfss
24. Huang, Q., Yang, L., Li, B., Du, H., Zhao, F., & Han, L. (2020). Cryptosporidium spp. and Giardia duodenalis emissions from humans and animals in the Three Gorges Reservoir in Chongqing, China. PeerJ, 1–27. https://doi.org/10.7717/peerj.9985
25. Johnson, K. A. (2013). A century of enzyme kinetic analysis, 1913 to 2013. FEBS Letters, 587(17), 1–39. https://doi.org/10.1016/j.febslet.2013.07.012
26. Kang, M. S., Park, J. H., & Kim, H. J. (2021). Predictive modeling for the growth of Salmonella spp. in liquid egg white and application of scenario-based risk estimation. Microorganisms, 9(486), 1–12. https://doi.org/https://doi.org/10.3390/microorganisms9030486
27. Kyakuwaire, M., Olupot, G., Amoding, A., Nkedi-kizza, P., & Basamba, T. A. (2019). How safe is chicken litter for land application as an organic fertilizer ?: A review. International Journal of Environmental Research and Public Health, 6(3521), 1–23.

https://doi.org/https://dx.doi.org/10.3390/ijerph16193521
28. Kyurkchiev, N., Markov, S., & Iliev, A. (2016). A note on the Schnute growth model. International Journal of Engineering Research and Development, 12(6), 47–54.
29. Li, D., Li, P., Yu, X., Zhang, X., Guo, Q., Xu, X., Wang, M., & Wang, M. (2021). Molecular characteristics of Escherichia coli causing bloodstream infections during 2010–2015 in a tertiary hospital, Shanghai, China. Infection and Drug Resistance, 14, 2079–2086.
30. Liu, S. (2017). How cells grow. In Bioprocess Engineering: Kinetics, Sustainability, and Reactor Design (2nd ed., pp. 629–697). Elsevier B. V. https://doi.org/10.1016/B978-0-444-63783-3.00011-3
31. Lobacz, A., Kowalik, J., & Zulewska, J. (2020). Determination of the survival kinetics of Salmonella spp. on the surface of ripened raw milk cheese during storage at different temperatures. International Journal of Food Science & Technology, 55, 610–618. https://doi.org/10.1111/ijfs.14315
32. Luka, Y., Kefas, H. M., Genza, J. R., & Abdul-hamid, B. A. (2014). Kinetics of bioremediation of Shinko drainage wastewater in Jimeta-Yola using Bacillus subtilis. International Journal of Engineering Research & Technology (IJERT), 3(3), 2429–2433. www.ijert.org 2433
33. Muloiwa, M., Nyende-byakika, S., & Dinka, M. (2020). Comparison of unstructured kinetic bacterial growth models. South African Journal of Chemical Engineering, 33, 141–150. https://doi.org/10.1016/j.sajce.2020.07.006
34. Nodar, R., Acea, M. J., & Carballas, T. (1990). Microbial composition of poultry excreta. Biological Wastes, 33(2), 95–105. https://doi.org/https://doi.org/10.1016/0269-7483(90)90150-Q
35. Pal, A., Bailey, M. A., Talorico, A. A., Krehling, J. T., Macklin, K. S., Price, S. B., Buhr, J., & Bourassa, D. V. (2014). Impact of poultry litter Salmonella levels and moisture on transfer of Salmonella through associated in vitro generated dust. Poultry Science, 100(8), 1–8. https://doi.org/10.1016/j.psj.2021.101236
36. Reynolds, J. (2016). Serial dilution protocols. American Society for Microbiology, 1–7.
37. Sanders, E. R. (2012). Aseptic laboratory techniques: Plating methods. Journal of Visualized Experiments, 1–18. https://doi.org/10.3791/3064
38. Shariful Islam, M., Kabir, K. M. A., Tanimoto, J., & Saha, B. B. (2021). Study on Spirulina platensis growth employing non-linear analysis of biomass kinetic models. Heliyon, 7, 1–9. https://doi.org/10.1016/j.heliyon.2021.e08185
39. Shukor, M. S., & Shukor, M. Y. (2014). Statistical evaluation of the mathematical modelling on the molybdenum reduction kinetics of a molybdenum-reducing bacterium. Journal Environmental Bioremediation and Toxicology (JEBAT), 2(2), 62–66.
40. Sieuwerts, S., Bok, F. A. M. De, Mols, E., Vos, W. M. De, & Vlieg, J. E. T. V. H. (2008). A simple and fast method for determining colony forming units. Letters in Applied Microbiology, 47, 275–278. https://doi.org/10.1111/j.1472-765X.2008.02417.x
41. Talaiekhozani, A., Jafarzadeh, N., Fulazzaky, M. A., Talaie, M. R., & Beheshti, M.

**International Journal of Research in Science & Engineering**
**ISSN: 2394-8299**
Vol: 01, No. 02, Oct-Nov 2021
http://journal.hmjournals.com/index.php/IJRISE
**DOI:** https://doi.org/10.55529/ijrise.12.1.24

(2015). Kinetics of substrate utilization and bacterial growth of crude oil degraded by Pseudomonas aeruginosa. Journal of Environmental Health Science and Engineering, 13(64), 1–8. https://doi.org/10.1186/s40201-015-0221-z

42. Tazdait, D., Abdi, N., Grib, H., Lounici, H., Pauss, A., & Mameri, N. (2013). Comparison of different models of substrate inhibition in aerobic batch biodegradation of malathion. Turkish Journal of Engineering & Environmental Sciences, 37, 221–230. https://doi.org/10.3906/muh-1211-7
43. Thomas, C., Idler, C., Ammon, C., Herrmann, C., & Amon, T. (2019). Inactivation of ESBL-/AmpC-producing Escherichia coli during mesophilic and thermophilic anaerobic digestion of chicken manure. Waste Management, 84, 74–82. https://doi.org/https://doi.org/10.1016/j.wasman.2018.11.028
44. Tuyarum, C., Meeboonlab, A., Tontikapong, K., & Lertworapreecha, M. (2019). Isolation and characterization of probiotic properties of lactic acid bacteria isolated from native chicken manure. SWU Science Journal, 35(2), 163–175.
45. UlukardeŞler, A. H., & Atalay, F. S. (2018). Kinetic studies of biogas generation using chicken manure as feedstock. Journal of Polytechnic, 0900(4), 913–917. https://doi.org/10.2339/politeknik.389622
46. Um-e-Habiba, Khan, M. S., Raza, W., Gul, H., Hussain, M., Malik, B., Azam, M., & Winter, F. (2021). A study on the reaction kinetics of anaerobic microbes using batch anaerobic sludge technique for beverage industrial wastewater. Separations, 8(43), 1–16. https://doi.org/https://doi.org/10.3390/ separations8040043 Academic
47. Van, D. P., Minh, G. H., Phu, S. T. P., & Fujiwara, T. (2018). A new kinetic model for biogas production from co-digestion by batch mode. Global Journal of Environmental Science and Management, 4(3), 251–262. https://doi.org/10.22034/gjesm.2018.03.001
48. Veys, O., Elias, O. S. De, Sampers, I., & Tondo, E. C. (2016). Modelling the growth of Salmonella spp. and Escherichia coli O157 on lettuce. 9th International Conference on Predictive Modelling in Food, 7, 168–172. https://doi.org/10.1016/j.profoo.2016.10.003
49. Widmer, G., Carmena, D., Kvá, M., Chalmers, R. M., Kissinger, J. C., Xiao, L., Sateriale, A., Stripen, B., Laurent, F., Lacroix-Lamande, S., Gargala, G., & Favennee, L. (2020). Update on Cryptosporidium spp .: highlights from the Seventh International Giardia and Cryptosporidium Conference. Parasite, 27(14), 1–10. https://doi.org/https://doi.org/10.1051/parasite/2020011
50. Xu, J., Tang, J., Jin, Y., Song, J., Yang, R., Sablani, S. S., & Zhu, M.-J. (2018). High temperature water activity as a key factor influencing survival of Salmonella Enteritidis PT30 in thermal processing. 509, 1–43. https://www.sciencedirect.com/science/article/pii/S0956713518305991